NUCLEAR SCIENCE AND ENGINEERING: **172**, 223–248 (2012)

Revisiting Insights from Three Mile Island Unit 2 Postaccident Examinations and Evaluations in View of the Fukushima Daiichi Accident

Joy Rempe*
Idaho National Laboratory, Idaho Falls, Idaho

Mitchell Farmer
Argonne National Laboratory, Argonne, Illinois

Michael Corradini
University of Wisconsin–Madison, Madison, Wisconsin

Larry Ott
Oak Ridge National Laboratory, Oak Ridge, Tennessee

and

Randall Gauntt and Dana Powers
Sandia National Laboratories, Albuquerque, New Mexico

Received January 13, 2012
Accepted March 26, 2012

Abstract—*The Three Mile Island Unit 2 (TMI-2) accident, which occurred on March 28, 1979, led industry and regulators to enhance strategies to protect against severe accidents in commercial nuclear power plants. Investigations in the years after the accident concluded that at least 45% of the core had melted and that nearly 19 tonnes of the core material had relocated to the lower head. Postaccident examinations indicate that about half of that material formed a solid layer near the lower head and above it was a layer of fragmented rubble. As discussed in this paper, numerous insights related to pressurized water reactor accident progression were gained from postaccident evaluations of debris, reactor pressure vessel (RPV) specimens, and nozzles taken from the RPV. In addition, information gleaned from TMI-2 specimen evaluations and available data from plant instrumentation were used to improve severe accident simulation models that form the technical basis for reactor safety evaluations. Finally, the TMI-2 accident led the nuclear community to dedicate considerable effort toward understanding severe accident phenomenology as well as the potential for containment failure.*

Because available data suggest that significant amounts of fuel heated to temperatures near melting, the events at Fukushima Daiichi Units 1, 2, and 3 offer an unexpected opportunity to gain similar understanding about boiling water reactor accident progression. To increase the international benefit from such an endeavor, we recommend that an international effort be initiated to (a) prioritize data needs; (b) identify techniques, samples, and sample evaluations needed to address each information need; and (c) help finance acquisition of the required data and conduct of the analyses.

*E-mail: joy.rempe@inl.gov

I. INTRODUCTION

On March 28, 1979, an accident occurred at the Three Mile Island Unit 2 (TMI-2) nuclear power plant. At the time of the event, many "believed—or maybe even hoped—that only minor damage had occurred in the core."[1] It was, however, 3 yr later before video examinations showed there was a large void in the upper core region, providing visual evidence that significant fuel damage had indeed occurred.[2] Following this revelation, the initially planned cleanup effort evolved into a research effort to learn from the "large scale experiment" that occurred at TMI-2 (Refs. 3 and 4).

Significantly greater understanding of severe accident progression and mitigation was available at the time of the events at the Fukushima Daiichi nuclear power station[a] than had existed at the time of the TMI-2 accident. A significant amount of this understanding was stimulated by TMI-2 examinations and evaluations. Modeling of boiling water reactor (BWR) accidents is quite different from modeling of pressurized water reactor (PWR) accidents. Thus, insights gained from TMI-2 activities on modeling of BWR accidents is at best indirect, and there is no comparable base of information available for BWRs. Focused examinations at Fukushima Daiichi can provide important new additional insights related to future research activities that could further enhance reactor safety.

I.A. Background

Although the TMI-2 accident involved severe damage to the reactor core, source terms to the containment differed dramatically from values assumed in licensing calculations. This called into question the accuracy of methods used to estimate source terms in earlier light water reactor (LWR) safety studies. In an effort to resolve these questions, four organizations, commonly referred to as the GEND Group—the GPU Nuclear Corporation, the Electric Power Research Institute (EPRI), the U.S. Nuclear Regulatory Commission (NRC), and the U.S. Department of Energy (DOE)—agreed to cooperate on reactor recovery and accident research.[3,4] The DOE research initially emphasized activities for reactor recovery (in those areas where accident recovery knowledge was of generic benefit to the U.S. LWR industry) as well as activities for severe accident technical data acquisition (such as the examination of the damaged core). Initial TMI-2 Accident Evaluation Program (AEP) efforts to collect, analyze, distribute, and preserve significant technical information available from TMI-2 were expanded to include research to gain an understanding of the sequence of events in the areas of core damage, high-temperature interactions between core components, and the behavior of fission products and materials. This expanded TMI-2 AEP effort included core damage progression analysis and metallographic studies of core debris samples and structural materials.

In support of the expanded TMI-2 AEP, an additional research program was formed under the auspices of the Committee on the Safety of Nuclear Installations of the Organisation for Economic Co-operation and Development (OECD). Under this program, several OECD countries and the European Communities' Joint Research Centre participated by performing detailed examinations of samples of fuel debris. However, it soon became apparent that the TMI-2 accident had progressed significantly further than originally believed.[5,6] Large quantities of molten core material had relocated from the core to the lower plenum of the reactor pressure vessel (RPV), and significant thermal damage had occurred to structures in the lower head region. Hence, the NRC proposed the establishment of a second international collaborative project, the TMI-2 Vessel Investigation Project (TMI-2 VIP), to examine additional aspects of the accident, such as "what potential modes of vessel failure were credible" and "what was the margin to failure for each mode." The condition and properties of material extracted from the lower head of the TMI-2 RPV were examined to determine the temperature conditions and the extent of the damage by chemical and thermal attack on the lower head, as well as the structural integrity margin of the RPV during the accident.

I.B. Motivation

Prior to the TMI-2 accident, a "Titanic mentality" (e.g., a sense of invulnerability) existed in many minds about nuclear reactor plant robustness because of conservatisms (e.g., redundant and diverse safety systems and barriers) included in the plant design.[2,3] This attitude, along with incomplete and inaccurate plant instrumentation, led industry and regulators to initially understate the severity of the accident.[7,8] Later, incomplete knowledge of the physical processes involved resulted in incorrect estimates of the potential for a hydrogen bubble to form, and its impact caused significant public anxiety during the event.[7,9] As discussed in this paper, unique information was obtained from TMI-2 postaccident evaluations related to PWR fuel degradation, relocation, interactions with structures, and relocated core debris coolability. Where additional data were needed to understand specific phenomena, such as materials-interaction phenomena, smaller-scale prototypic experiments were performed in well-controlled conditions (e.g., see Ref. 10). Combined insights from TMI-2 and these smaller-scale tests are today embodied in severe accident analysis simulation models.

Significantly more information related to severe accident progression and mitigation was available on March

[a]Hereinafter, the Fukushima Daiichi nuclear power station is referred to simply as "Fukushima Daiichi."

11, 2011 (when the events occurred at Fukushima Daiichi) than at the time of the TMI-2 accident. Increased understanding about BWR severe accident phenomena and accident progression allowed plant staff at the Fukushima Daiichi reactors to understand and, to some extent, predict the observed phenomena. For example, it was understood that decreased water levels would cause fuel oxidation and hydrogen production. Although efforts to vent the hydrogen were handicapped by several unexpected difficulties,[11,12] it was clear that plant staff understood what actions were required to mitigate the accident consequences. Nevertheless, significant issues still arose due to incomplete information about the water level, pressure, and temperatures in the core and containment; among the issues were the potential for RPV head and/or penetration failure, the status of the spent-fuel pools (SFPs), and possible hazards associated with salt water addition. This lack of accurate data and incomplete understanding about the status of the plants led to incorrect statements by plant management and public officials.

Released data[11,12] suggest that three of the BWRs at Fukushima Daiichi experienced core damage. Prior evaluations[13] indicate that the loss of power and adverse conditions in these three reactors would adversely impact the accuracy of BWR plant sensor data (e.g., pressure gauges, water-level sensors, and thermocouples were exposed to conditions beyond their operating envelope). Reports[14,15] indicate that Tokyo Electric Power Company is obtaining visual images inside the containment vessel of the Fukushima Daiichi Unit 2 (Unit 2) reactor; ultimately, the fuel will be removed from Fukushima Daiichi Unit 1 (Unit 1), Fukushima Daiichi Unit 3 (Unit 3), and Unit 2, as was done at TMI-2. We believe that it is essential to also obtain samples and perform the associated analyses so that BWR accident progression knowledge and safety analysis models can be enhanced to a level commensurate with PWR models that were improved using data obtained from the TMI-2 postaccident examinations.

As discussed in this paper, limited data are available to characterize the heatup and degradation of BWR fuel, cladding, and other core structures (channel walls and control blades), melt relocation, and the effectiveness of accident mitigation measures. As discussed in Sec. III, BWR models are based on a significantly smaller number (approximately ten) of small-scale tests with prototypic materials. These models are, in general, much less validated than PWR-specific severe accident models, which are based on more than 40 tests. We observe that BWR models are essentially limited to in-core structural degradation phenomena. The interaction of melt with the BWR core plate and the behavior of melt/debris with the large volume of water in the lower head and the steel structures (~100 tons) within the BWR bottom head have never been experimentally studied. Likewise, no prototypic data exist for modeling BWR RPV failure. Last, if failure occurred in any of the RPVs at Fukushima Daiichi, there may be an opportunity to obtain real-scale data for evaluating ex-vessel phenomena that are applicable to BWR and PWR containments. Hence, data and analyses from Fukushima Daiichi have the potential to fill BWR and ex-vessel phenomena data gaps, thereby increasing the knowledge base supporting reactor safety technologies, and have a beneficial impact on the safety of reactors internationally.

I.C. Objectives and Organization

As a first step to gain support for an effort to obtain data from the reactors at Fukushima Daiichi, we have prepared this paper with the following objectives: first, summarize important data and insights obtained from TMI-2 postaccident evaluations; second, summarize what experimental data are currently available to support severe accident simulation tools; and third, identify what data could be obtained from Units 1, 2, and 3 to further enhance LWR safety. We recommend that an international program be established to develop a consensus on what knowledge and information should be gleaned for various possible end states at these reactors and to fund completing postaccident evaluations.

Sections II, III, and IV each address one of the objectives. Section II highlights what information was gained from the TMI-2 postaccident evaluations, Sec. III reviews the current data available to validate severe accident simulation models and identifies gaps in data for predicting in-vessel and ex-vessel severe accident progression, and Sec. IV emphasizes what knowledge gaps can be closed by examinations at Units 1, 2, and 3. Finally, Sec. V provides a summary along with recommendations for steps that can be taken to maximize the benefits of postaccident analyses.

II. TMI-2 ACCIDENT SCENARIO AND POSTACCIDENT EVALUATIONS

Numerous insights were gained from the TMI-2 postaccident evaluations. Initially, evaluations were used to assess the accuracy of available plant instrumentation and improve accident simulations. As additional data from postaccident evaluations became available, descriptions of the accident were clarified, and accident simulation models were improved, where needed. Although there is still some debate about certain aspects of the TMI-2 accident,[16] the information obtained from the postaccident evaluations and enhanced models provided a basis for improving plant design features, operator training, and accident mitigation strategies. In this section, TMI-2 design features, available instrumentation data, and accident sequence events are summarized. Then, an overview is provided of the data, examinations, and analyses completed with important insights obtained from these

postaccident examinations. This information is included in this paper as an example that emphasizes that initially incomplete and inaccurate plant instrumentation data, coupled with insights obtained from postaccident examination data, can provide important information required for improving reactor safety.

II.A. Plant Description and Instrumentation Data

The TMI-2 reactor was a PWR designed and manufactured by Babcock & Wilcox, Inc. The core contained 177 fuel assemblies, corresponding to 93.1 tonnes of fuel. The fuel was designed for a maximum local burnup of 55 000 MWd/tonne U. At the time of the accident, the burnup ranged from 900 to 6000 MWd/tonne U (Ref. 17). Core reactivity was controlled with control rod assemblies containing silver-indium-cadmium alloy as well as boron dissolved in the coolant. Reactivity was also controlled with burnable poison rod assemblies for the first fuel cycle. There were 52 instrument assemblies in the core. Each assembly contained several self-powered neutron detectors (SPNDs), one gamma-compensating background detector, and one Type K (chromel-alumel) core exit thermocouple. In addition, three source range monitors (SRMs), which were located outside the RPV, provided a means for monitoring reactor operation. The reactor coolant system (RCS) consisted of the RPV, two vertical once-through steam generators, four shaft-sealed reactor coolant pumps, an electrically heated pressurizer, and interconnecting piping. The system was arranged with two heat transport loops, each with two pumps and a steam generator (often designated as the A and B loops).

Plant instrumentation provided initial information related to the timing of accident progression. Available TMI-2 sensor data (shown in Fig. 1) include source and intermediate-range counter rate, reactor coolant pump operation, reactor coolant flow, high-pressure injection pump operation, reactor coolant outlet temperature, core flood injection, reactor inlet temperature, pilot operator relief valve (PORV) block valve operation, and reactor coolant pressure. A TMI-2 analysis exercise was completed in conjunction with the TMI-2 AEP to assess the accuracy of such data and update modeling tools.[18] In addition to providing data for model assessment, the data (see Fig. 1) provide a reference for understanding the accident scenario summarized in Sec. II.B.

As part of the postaccident evaluations, plant sensors were deployed in nontraditional ways to gain insights about the final state of materials within the TMI-2 RPV (Ref. 19). For example, estimates for core materials in the lower head were informed by results from ion chamber scans of in-core instrumentation calibration tubes,[20] electrical resistance measurements of thermocouples (to determine their remaining lengths),[21] and neutron dosimeter measurements (to detect uranium distribution).[22] Mechanical probes were also used to determine the depth of loose debris and elevations of resolidified molten material or crust at locations below the core cavity and in the core bypass region, and the location of plugs in the in-core instrumentation calibration tubes.[23]

II.B. Overview of Accident Scenario

Numerous references provide descriptions of the TMI-2 accident sequence.[6,19,24,25] It should be noted that such descriptions were informed and updated as TMI-2 AEP results became available. The scenario defined at the end of the TMI-2 postaccident examinations is presented in this section. As noted within this and subsequent sections, many details pertaining to the core heatup and relocation scenario could only be obtained from postaccident examinations and testing.

The TMI-2 accident was initiated by a shutdown of secondary feedwater flow caused by a trip of the condensate booster pumps and then the feedwater pumps, during attempts to unclog a pipe leading from the full-flow demineralizers downstream of the condenser. Following turbine isolation (defined as time "0" in Fig. 1) and reactor trip (when reactor pressure reached 16.3 MPa at 10 s after turbine trip), the steam generator boiled dry, and the resultant reduction of primary-to-secondary heat exchange caused the primary coolant to heat up, surge into the pressurizer, and increase the primary system pressure. The PORV opened to relieve pressure when the RCS pressure reached 15.7 MPa (Ref. 24). The PORV failed to close when RCS pressure decreased. The first 100 min of the accident can be characterized as a small-break loss-of-coolant accident (SBLOCA) with resultant loss of primary coolant and decreasing pressure. The event differed from a typical SBLOCA in that the pressurizer liquid level remained high. This was incorrectly interpreted by the reactor operators[6,24] as indicating that the RCS was nearly full of water, when in fact, the RCS was continually losing its water inventory. Emergency core cooling was reduced by operators to address their concerns about a full RCS. However, the coolant void fraction increased because of coolant loss through the PORV and decay heat generation by the fuel. The steam inventory in the primary system piping increased to such an extent that RCS pumps were tripped by the operators to prevent permanent damage from pump cavitation after 100 min (Refs. 6 and 24).

At the time that pump operation ceased (see Fig. 1), increases in the SRM count rate and coolant system temperature and pressure suggest that the RPV liquid level decreased. Studies correlating the response of the SRMs with the core liquid level suggest that core uncovery began between 114 and 120 min and reached the core midplane by ~140 min (Refs. 6 and 25). Insufficient decay heat removal associated with core uncovery is estimated to have led to upper regions of the

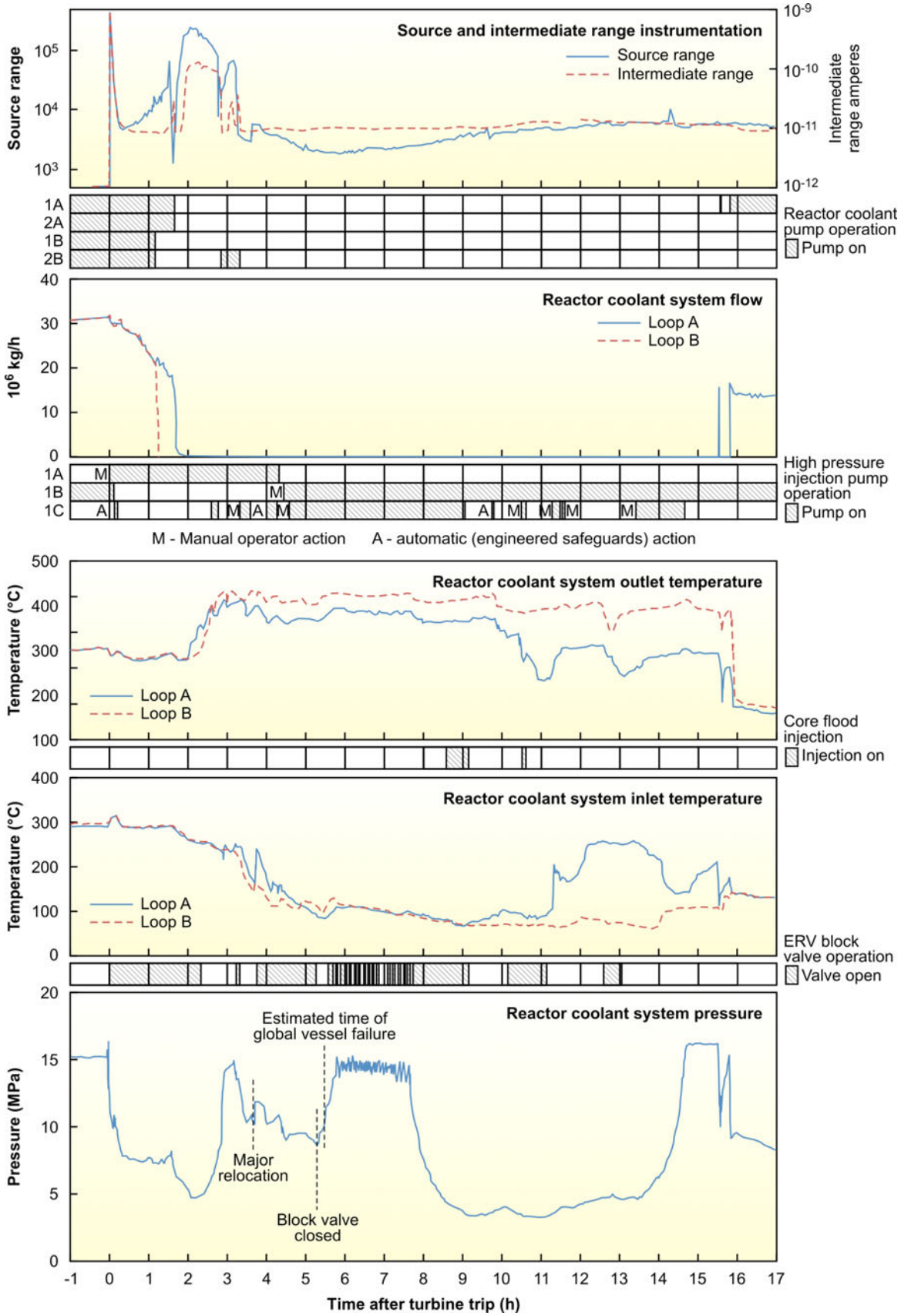

Fig. 1. TMI-2 data from March 28, 1979 (Ref. 6).

core heating to temperatures that cause cladding to overheat, balloon, and rupture.[25,26] Such cladding failure, which results in the release of gaseous fission products, was substantiated by significant increases in containment radiation levels at 140 min. When operators finally realized that the PORV was failed in the open position, they closed the pressurizer block valve upstream of the PORV, terminating coolant loss and the release of fission products to the containment.

In-core SPND output and RCS pressure (see Fig. 1) indicate that core temperatures continued to increase between 150 and 165 min. Subsequent analysis of the SPND output indicated that temperatures probably reached 1077°C (Ref. 27). Insights gained from materials interaction and severe accident testing (e.g., see Refs. 10 and 28) suggest that Zircaloy-steam exothermic reaction initiated, producing large amounts of hydrogen, reducing heat transfer to the secondary side in the steam generator, and dramatically increasing the core heatup rate. Zircaloy melting temperatures were exceeded, resulting in relocation of the molten Zircaloy and some liquefied fuel to the lower core regions, solidifying near the coolant interface. This continued until 174 min, when a dense agglomeration of degraded core material formed in the lower central regions of the core and blocked steam flow through the core.

At 174 min (see Fig. 1), one of the reactor coolant pumps in the B loop was turned on for ~19 min, and coolant was pumped into the RPV. This coolant injection rapidly repressurized the RCS. Core exit thermocouples above peripheral fuel assemblies indicate that cooling occurred, and the SRM count rate decreased at the time of this injection (see Fig. 1). Several references[24,25,29] indicate that the thermal-mechanical forces resulting from this injection and follow-on rapid steam formation may have shattered the oxidized fuel rod remnants in the upper regions of the core, forming a rubble bed on top of the consolidated core materials. At 200 min, the high-pressure injection system was operated for 17 min. The RPV was refilled with water by ~207 min.

Although the core was estimated to have been covered with coolant, analyses suggest that little coolant was able to penetrate the consolidated core region and that these materials continued to heat up.[26] Between 224 and 226 min after reactor scram, plant instrumentation (RCS pressure increase, SRM count rate increase, cold-leg temperature increase, and in-core SPND increase) indicated that the outer crust (resolidified molten material) surrounding the relocated core material failed, and molten core material relocated to the lower plenum.[6,24,25] The pressure rise between 224 and 240 min indicates that steam generation was significant for at least 15 min. The operators repeatedly cycled the pressurizer block valve between 320 and 480 min, transferring coolant to the containment building. Increases in the SRM count rates (see Fig. 1) suggest that small quantities of molten debris may have continued to relocate to the lower head between 230 min and 15.5 h, although peak count rates are considerably lower than the values during the 224- to 226-min relocation time period. At 15.5 h, one of the A-loop primary coolant pumps was restarted, reestablishing heat removal from the RPV.

II.C. Insights from Video and Ultrasonic Exams

Throughout the TMI-2 postaccident examination program, video inspections provided new insights about the end state of the relocated debris, the damage to structures, and the melt relocation process. In 1982, quick-look video surveys using closed-circuit television camera inspections of the core were initiated.[4,30] After discovering that a large void existed in the upper core region, the plant staff attempted to insert all eight axial power shaping rod (APSR) assemblies, but insertion depths at several locations were much shorter than expected. Only one of the eight APSRs could be inserted their normal depth of 94 cm; insertion depths for four of the APSRs were <25 cm (Ref. 31). In 1983, ultrasonic scanning surveys were used to determine the shape and dimensions of materials remaining in the core cavity.[32] These surveys indicated that the voided cavity volume was ~26% of the original core region. Additional video surveys,[33] obtained after the RPV head and plenum assemblies were removed, provided evidence of regions where damage to the lower head guide tube and penetration structures was more severe, and a crack in the RPV cladding near an instrumentation tube was identified (see Fig. 2). Ultimately, information obtained from video examinations, ultrasonic surveys, and other inspection techniques was used to develop maps indicating the damage to core support structures and the location of the remaining core materials.[19]

II.D. Sample Examination

TMI-2 postaccident examinations included several activities[4,6] to extract and evaluate samples from the RPV. Debris samples included debris grab samples from the core rubble bed, fuel rod segments, core stratification samples, distinct fuel assembly and control rod cluster components (e.g., cladding, control rods, spiders, spacer grids, end fittings, and hold-down springs), and in-core instrumentation and debris from the lower RPV. Fuel removal was initiated on November 12, 1985. A total of 23 000 kg (51 000 lb) of the 140 000 kg (300 000 lb) of the core material was removed, including upper end fittings from the fuel, control rod, and burnable poison rod assemblies; partial fuel assemblies; and loose debris. In addition, samples were extracted from the RPV upper and lower plenums, the primary RCS piping and vessels, and the TMI-2 equipment and buildings external to the primary RCS. Sample examinations applied a variety of metallurgical, chemical, and radiochemistry methods.

Fig. 2. Photo of the H8 instrumentation nozzle with crack on RPV cladding (Photo courtesy General Public Utilities).

As part of the TMI-2 VIP (Ref. 6), examinations were performed on samples from the cohesive layer of debris next to the RPV, often referred to as the "companion" debris samples. In addition, the TMI-2 VIP included removal and examination of RPV steel, nozzle, and guide tube samples. In removing the companion debris samples, it was observed that this dense layer of debris was extremely hard and that it had to be broken into pieces for removal. However, there was virtually no adherence of the material to the lower head.[34,35] Electrical discharge machining methods were used to cut 15 prism-shaped metallurgical "boat samples" of steel from the RPV lower head,[36] and examinations[37] were performed at U.S. and OECD partner laboratories to determine the peak temperatures experienced by the steel, the duration of these peak temperatures, and the subsequent cooling rate for the steel. Optical metallographic and hardness tests[38] were performed on RPV steel to estimate the maximum temperature various portions of the lower head reached during the accident. Creep and tensile tests[37] provided insights about changes in material properties after this steel experienced elevated temperatures. Metallurgical examinations[39] were also performed on RPV steel samples with cracked cladding overlayer material. Nozzle and guide tube examinations[40] included microphotography and macrophotography, optical metallography, scanning electron microscope measurements, gamma scanning, melt penetration measurements, and microhardness measurements.

Several other TMI-2 components were also examined as part of the TMI-2 AEP (Ref. 41). For example, one major activity was to characterize surface deposits and peak temperatures experienced at locations other than the core region, such as RCS components and structures, control rod leadscrews, leadscrew support tubes, plenum cover debris, resistance thermal detector thermowells, steam generator manway cover backing plates, and makeup and letdown system filters. In addition, samples were obtained from locations in the reactor building, such as basement sediment and reactor coolant drain tank contents.

II.E. Phenomenological Insights

Significant insights related to phenomena occurring during the TMI-2 accident include the following:

1. All TMI-2 fuel assemblies were damaged. Large regions of the core exceeded the melting temperature of the cladding (~1900°C). Significant fuel liquefaction by melted Zircaloy and some fuel melting occurred (corresponding to peak temperatures of at least 2800°C).

2. Approximately 20% of the core materials escaped from the core as a liquid phase and solidified in lavalike formations in the core bypass region, the core support assembly (CSA), and the RPV lower head region. The estimated damage and core end-state configuration is summarized in Table I (Ref. 19).

3. Based on the end-state core and CSA configuration and supporting analysis of core heatup, it is believed that the crust (or resolidified molten material) surrounding the relocated core material (see Sec. II.B) failed near the top of the molten core region in the southeast quadrant of the RPV. Limited damage to the CSA

TABLE I

Estimated Final State of Material Within TMI-2 RPV*

Region	Percent Core Material
Cavity in upper core region	26% voided[a]
Standing but damaged fuel assemblies or fuel assembly stubs	33%
Loose (unmelted and previously molten core material mixture) debris below the cavity in the upper core region	20%
Previously molten core material	47%
Retained in core boundary	25%
Escaped from core boundary	22%
Core bypass region	3%
CSA	4%
Lower plenum[b]	15%

*Reference 19.
[a]Not included in core material total.
[b]Between RPV lower head and CSA.

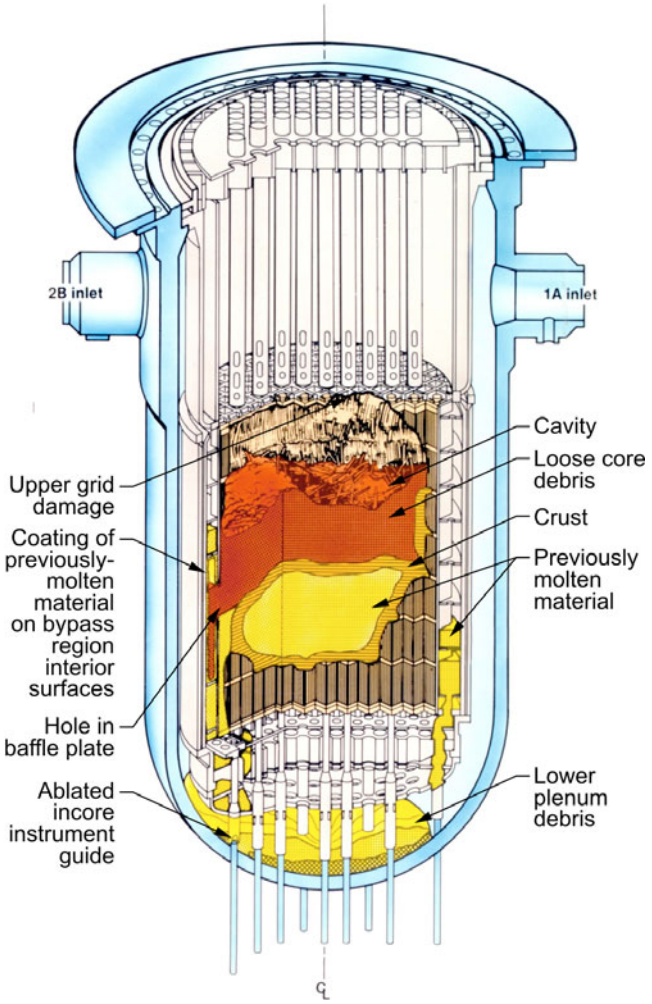

Fig. 3. Postulated final state of materials within the TMI-2 RPV (Ref. 6).

occurred as the core material flowed to the lower plenum. Figure 3 illustrates the final state of materials within the TMI-2 RPV based on available instrumentation, analyses, and postaccident examinations.[25]

4. Metallurgical examinations of the boat samples in conjunction with visual observations suggest that an elliptical region of the RPV, ~0.8 × 1.0 m, reached peak temperatures of 1100°C during the accident (see Fig. 4). Note that this peak temperature was well above the steel's transition temperature of 727°C, where ultimate strength is significantly reduced (due to the transition from ferritic to austenitic steel). At 5 cm below the inner surface of the RPV, peak temperatures were at least 100°C ± 50°C lower.[37,38] Examinations[38] indicate that the steel may have remained at peak temperatures for as long as 30 min before cooling occurred. Cooling rates of 10°C to 100°C/min were inferred[37,38] from examinations. At locations away from the hot spot, there is no evidence to indicate that RPV steel temperatures exceeded 727°C (Refs. 37 and 38).

5. Metallurgical examinations of cracks or "tears" in the RPV cladding (see Fig. 2) in samples taken near the hot spot (positions E-6 and G-8) indicate that the damage extended down to, but not into, the carbon steel RPV (Ref. 39). Cracks were typically found near nozzles. Examinations[39] indicate that these cracks were due to differential thermal expansion between the stainless steel cladding and the carbon steel RPV. Metallurgical examinations[39] support the conclusion that the tearing was due to differential thermal expansion when these materials were subjected to rapid cooling (at rates from 10°C to 100°C/min). Furthermore, the presence of control material within the cladding tears indicates that control material relocated to the lower head prior to the time when the primary relocation of reactor fuel occurred.

6. Nozzle damage (see Fig. 5) was caused by molten core material relocating to the lower head.[40] The most severe damage was observed in nozzles located within the hot spot region of the RPV. Examinations indicate that the observed damage was not related to the embedded debris height (e.g., nozzle L6 was submerged in debris but remained undamaged). Partially melted nozzle stubs indicate that peak temperatures were as high as 1415°C, the liquidus temperature for INCONEL® alloy 600.[b] Surface scale found on the nozzles below their

[b]INCONEL is a registered trademark of the Special Metals Corporation group of companies.

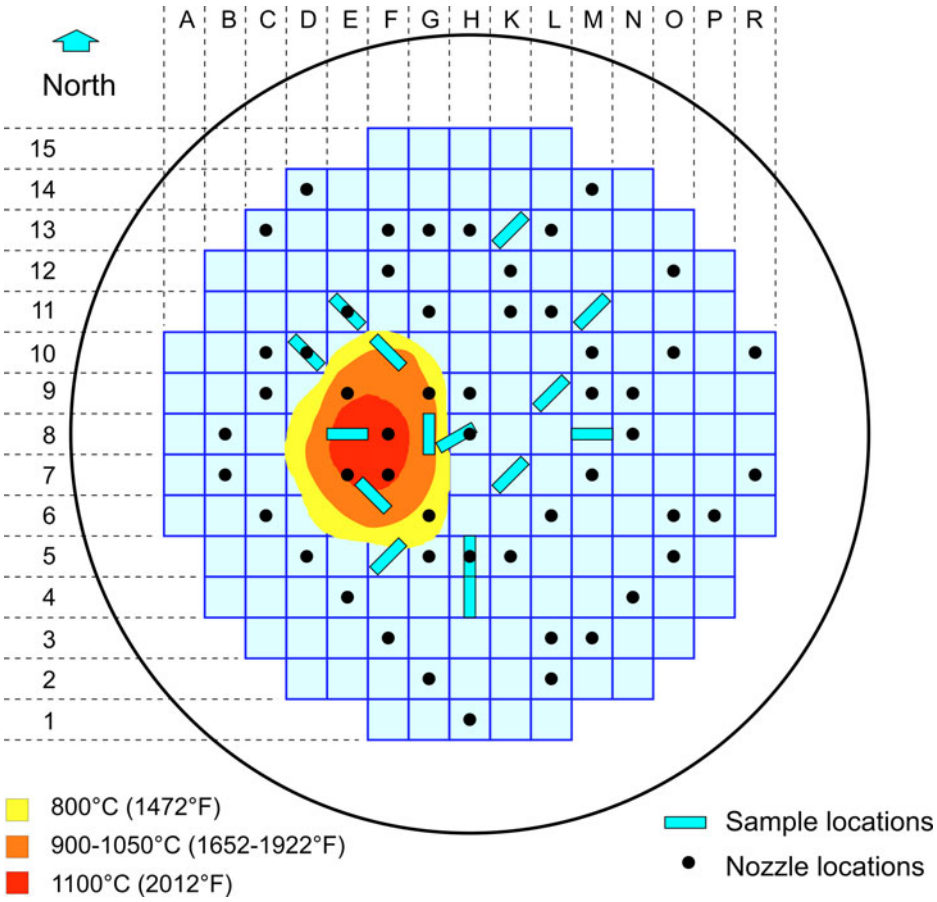

Fig. 4. Location of TMI-2 RPV boat samples and hot spot.[6]

meltoff points suggests that molten material flowed on top of a crust of preexisting solidified fuel debris. In fact, lower portions of the nozzles appear to have been protected by crusts that rapidly formed near RPV surfaces. Maximum fuel penetration depths observed within the nozzles indicate that melt could not relocate to depths below the lower head thickness. Examinations also indicate that Ag and Cd were present on nozzle surfaces, suggesting that control material relocated prior to the primary fuel relocation.

7. Approximately 7 kg of the 19 000 kg of debris that relocated to the lower head was examined to develop estimates of debris decay heat in relocated material. It should be noted that only the quadrant from where the samples were taken was known and that the hard layer had to be broken into pieces as part of the acquisition process. Nevertheless, examination results yielded consistent values for all of the samples examined.

With respect to the proposed Units 1, 2, and 3 examinations, it is worth noting that many of the above insights were gained from the smaller TMI-2 VIP effort that was funded by OECD when funding for GENP was no longer available. Although no systematic evaluation was performed with respect to the benefit versus the cost of extracting and examining various types of samples from TMI-2, it is recognized that proposed Unit 1, 2, and 3 examinations should be cognizant of funding limitations and prioritize efforts according to their potential impact.

III. LWR SEVERE ACCIDENT PROGRESSION KNOWLEDGE

The realization by industry[2,3] and regulators[1] that severe accidents with substantial core degradation were credible led to increased research efforts by organizations such as EPRI, DOE, and NRC to acquire a basic knowledge of the progression and consequences of a wide range of risk-dominant severe accidents. In-vessel research[42–44] focused primarily on fuel damage tests, radionuclide release and transport, melt-water

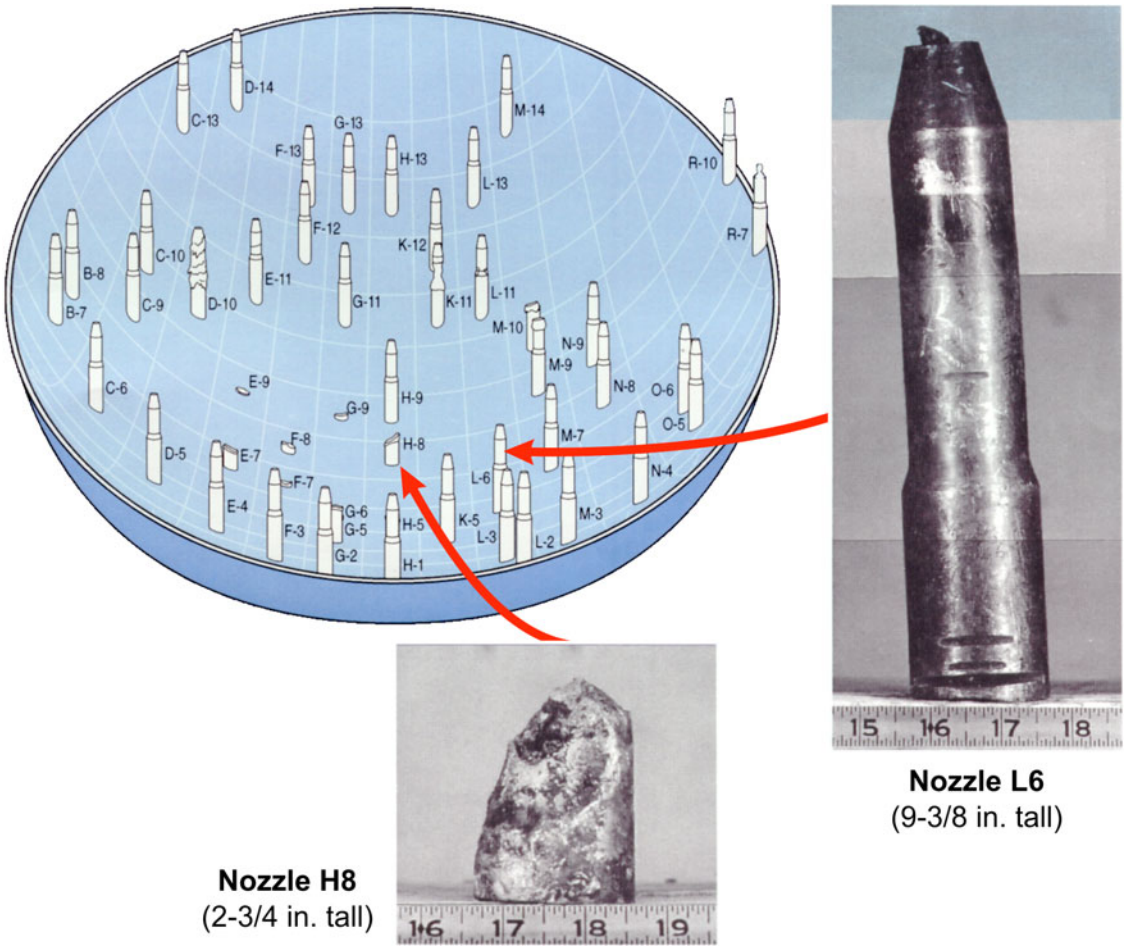

Fig. 5. End state of nozzles on the TMI-2 RPV lower head.[6]

interactions, melt relocation, and RPV failure evaluations. Ex-vessel research[43] focused primarily on containment integrity and radionuclide release and transport, addressing identified phenomena with the potential to lead to early containment failure (i.e., within the first 2 h after RPV breach within an accident). These phenomena include hydrogen combustion, steam explosions, direct containment heating, bypass due to steam generator tube failures or penetration isolation failures, and melt attack on the BWR Mark I containment liner. Considerable research[43] was also performed to gain insights about phenomena that could lead to late containment failure, such as molten core–concrete interactions (MCCIs), as well as aspects of "early containment failure phenomena" that could also lead to late failures (e.g., hydrogen combustion, Mark I liner failures, etc.). Insights gained from such evaluations are embedded in analytical models. This section highlights the capabilities of U.S. systems analysis codes for predicting severe accident progression and data for assessing selected phenomena simulated within these codes. The phenomena described in this section were selected to highlight gaps that data from Fukushima Daiichi Units 1, 2, and 3 could fill.

III.A. U.S. Severe Accident Systems Analysis Tools

Over the decades, researchers embedded their knowledge related to severe accident progression into analysis tools. In the United States, most researchers currently rely on the MELCOR (Ref. 45) or Modular Accident Analysis Program (MAAP) (Ref. 46) systems analysis codes to predict severe accident progression. The industry-developed MAAP code models RCS thermal hydraulics, core melting and relocation, fission product release and transport, RPV failure, and containment failure. Industry organizations have relied on MAAP analyses to complete Individual Plant Examinations and severe accident mitigation evaluations. The MELCOR code encompasses all of the phenomena modeled by MAAP. It is a fully integrated, engineering-level computer code whose

primary purpose is to model accident progression in current nuclear power plants, new and advanced reactor designs, and some nonreactor systems such as SFPs. The severe accident codes discussed in the above paragraphs were developed in the United States; there are also several other internationally developed codes available, notably IMPACT/SAMPSON, ICARE2/CATHARE, ATHLET/CD, and the SVECHA package (Refs. 47, 48, 49, and 50, respectively).

Figure 6 compares phenomena modeled by MAAP and MELCOR with U.S. codes that were previously used to predict selected aspects of severe accident phenomena. The SCDAP/RELAP5 severe accident systems analysis code[51] models in detail the primary RCS, fuel heatup, degradation, and relocation, while the CONTAIN code[52] focuses on containment system phenomena. The detailed VICTORIA code[53] predicts the chemical forms of fission products in the primary RCS. The original MELCOR code was developed by the NRC to support Level 2 probabilistic risk analysis efforts. It included models for the reactor core, RCS, and safety systems as well as containment systems in a less detailed manner than more mechanistic thermal-hydraulic and fuel rod codes. Recognizing the importance of an integrated analysis tool, the NRC consolidated the physical models and capabilities of more detailed severe accident codes into MELCOR. This consolidation effort is designed to ultimately provide an efficient state-of-the-art code for severe accident analyses to support plant design certifications and risk-informed regulatory decisions related to plant modifications.

Prior to the TMI-2 accident, the accepted method for analyzing releases from postulated accidents invoked the use of deterministic analyses and assumptions that were deemed conservative. The TMI-2 accident raised doubts about the soundness of this practice.[54] For example, the fact that failure of the RPV head or its penetrations did not occur after nearly 19 tonnes relocated to the lower head was inconsistent with predictions from modeling tools available at the time of TMI-2. Furthermore, the amount and chemical form of iodine releases to the containment differed significantly from source terms assumed in licensing calculations. Currently used U.S. severe accident codes (that were not in existence at the time of the TMI-2 accident) have been considerably improved by obtaining additional data for model development and validation. However, as noted previously, enhancements have primarily reduced uncertainties related to in-vessel PWR accident progression phenomena. Examinations of samples obtained from Fukushima Daiichi may provide real-scale data for assessing BWR and PWR ex-vessel models in addition to BWR in-vessel models.

III.B. Data for Systems Analysis Code Validation

Data for model development and validation are essential for estimating and reducing, if needed, the uncertainty of severe accident analysis code predictions. To illustrate the process, we discuss in this section three types of phenomena simulated in MELCOR and MAAP with available data to support development and validation of models simulating these phenomena. Phenomena were selected to highlight gaps that data from Fukushima Daiichi could fill.

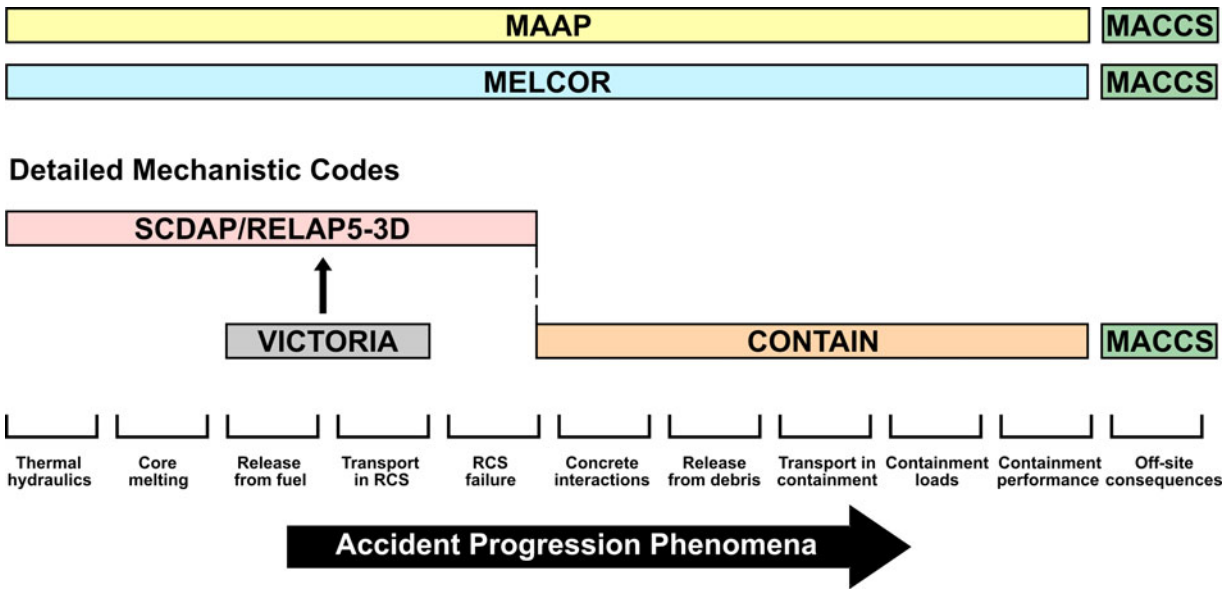

Fig. 6. Severe accident phenomena modeled by MAAP, MELCOR, and other U.S.-developed codes.

III.B.1. In-Vessel Phenomena

As noted above, in-vessel severe accident analysis results are dominated by models that predict core heatup, degradation, and relocation and radionuclide release and transport. Reflooding and quenching of degraded fuel materials have also been shown to significantly impact accident progression. Table II summarizes experimental data used to develop and validate models of in-vessel phenomena. As indicated in Table II, the data are primarily from smaller-scale experiments (with the exception of TMI-2 data). Furthermore, there are fewer BWR tests (~10) than PWR tests (~40).

To gain insights about the uncertainties in the capability of severe accident codes to predict PWR core degradation phenomena, the OECD/Nuclear Energy Agency completed a study to assess the capabilities of the state-of-the-art computer codes in predicting the severe accident progression for a well-defined representative SBLOCA in TMI-2 (often referred to as the "alternative TMI-2 accident scenario").[61] MELCOR 1.8.6, MELCOR 1.8.5, MAAP 4, and several other codes developed by foreign organizations were evaluated. In general, the predictions for many parameters, especially those related to system thermal-hydraulic conditions, core degradation up to reflood, and hydrogen production, were in relatively good agreement. This is attributed to the fact that over the last two decades, these codes were assessed using the same integral tests and that experienced code users prepared the input models. However, the scatter in code predictions for some phenomena (for which physical understanding is still incomplete) revealed some model weaknesses. The largest discrepancies were observed during the reflooding phase. Although there was general agreement on the calculated pressure increase, hydrogen production, and the increased rate in degradation, code predictions differed on the calculated efficiency of quenching. In general, most differences were attributed to the need for additional experimental data and improved understanding of the phenomena. Nevertheless, this benchmark exercise demonstrated that simulation tools have been significantly improved over the last two decades and that code-to-data assessments were beneficial in reducing modeling uncertainties related to PWR in-vessel phenomena. This reduced level of uncertainty increased industry and regulator confidence in code predictions related to PWR severe accident management (SAM) measures such as primary system depressurization, delayed start of high-pressure core injection, and loss of emergency feedwater system. Similar benefits may be obtained from examinations of fuels and structural materials within the RPVs at Units 1, 2, and 3.

III.B.2. Late-Phase Accident Progression

As indicated in Table III, prototypic data for predicting late-phase accident phenomena such as melt relocation and RPV failure are more limited than the data for predicting early-phase accident phenomena. Data from prototypic experiments [fuel melt and release oven (FARO), RASPLAV, MASCA, and Fission Product Test (FPT)-4 (FPT-4)] for simulating melt relocation and molten pool behavior do not include prototypic structures encountered in nuclear power plants. Likewise, RPV and penetration failure testing [lower head failure (LHF) and OECD LHF (OLHF)] were small-scale tests focused on PWR RPV geometries (typically an ~14-cm lower head with 50 to 60 ~3- to 5-cm–diam instrument tube penetrations), and the materials and geometry considered only single instrumentation tube configurations. This situation differs considerably from the thicker lower heads of BWR RPVs (~21 cm), which have INCONEL alloy 600 or stainless steel cladding with 55 instrument tubes (5- to 6-cm–diam), 185 control rods (there are ~100 tons of these ~12-cm-diam structures in the bottom head of a Browns Ferry class reactor), and a drain line (6-cm outer diameter).

Although data from the TMI-2 accident provide insights needed to extrapolate such small-scale data to PWR evaluations, differences in BWR lower head structures make such extrapolations more difficult to justify. For example, there is considerably more mass associated with BWR internal structures and components, such as the thick core support plate and lower head penetrations, relative to PWR designs; plus, all BWR RPV designs include "skirts" on the lower RPV head that support the RPV on the concrete pedestal/biological shield within the drywell. It should be noted that none of the LHF tests included a skirt-supported RPV or penetrations representative of the 185 larger-diameter (nearly 12-cm) control rod drive penetrations typically found in BWR plants. External lower head structures, such as the control rod drives, can act as "fins" to remove heat from the lower head, which may delay RPV breach as well as locations where melt can breach welded joints and cause some molten corium material release. Given a RPV breach, corium melt may fragment and refreeze when spilling into a "maze" of metal structures. Some of these external metal components may melt and be added to the corium mass, possibly slowing down any corium relocation from the lower pedestal region and delay containment failure. The addition of more metal to the corium may also affect subsequent accident progression phenomena, such as MCCI and fission product release and distribution. Finally, if water is present below the RPV, any RPV failure from corium melt relocation presents a potential for an energetic fuel-coolant interaction that must be considered, as it affects corium debris formation and local pressurization.

III.B.3. Ex-Vessel Assessment Data

Ex-vessel research[43] has focused on evaluating the nature and extent of the MCCI and concurrent fission

TABLE II

Core Heatup, Degradation, and Fission Product Release Data*

Test/Accident	Description	Phenomena Tested
PWR		
Loss-of-Fluid Test		
FP-2	Large-scale fuel bundle severe damage test with reflood	Fuel heatup (temperatures) and damage, cladding oxidation, H_2 generation, quench behavior
Power Burst Facility Severe Fuel Damage		
SFD ST	Heatup of PWR fuel assembly; top of fuel assembly uncovered due to coolant boiloff	Boiloff rate, temperature and fuel rod damage, H_2 production
SFD 1-1	Small-scale bundle heatup with unirradiated fuel; steam flow through assembly	Temperature and fuel rod damage, H_2 production
SFD 1-4	Small-scale bundle heatup with irradiated fuel rods included; helium quench phase	Fuel heatup (temperatures) and damage, H_2 generation
SNL Annular Core Research Reactor		
MP series	Small-scale simulation of the heatup of PWR in-core debris bed, formation of melt pool and crust	Debris bed melting, formation of ceramic crust, melt pool growth, reformation of crust
ST series	Small-scale fission product release experiments from irradiated Zircaloy-clad fuel	Fission product release from irradiated fuel
Full-Length, High-Temperature		
FLHT-2	Heatup of full-length PWR fuel assembly; coolant boiloff	Boiloff rate, fuel heatup (temperatures) and damage, H_2 generation
FLHT-4	Heatup of full-length PWR fuel assembly; coolant boiloff	Boiloff rate, fuel heatup (temperatures) and damage, H_2 generation, noble gas release
FLHT-5	Heatup of full-length PWR fuel assembly; gradual boiloff of coolant; most severe of the FLHT tests	Boiloff rate, fuel heatup (temperatures) and damage, H_2 generation, noble gas release
CORA		
CORA-2	Small (23 rods) fuel assembly with electrical heater rods, INCONEL alloy 600 spacers, reference test, 1987	Fuel heatup (temperatures) and damage, cladding oxidation, H_2 generation
CORA-3	Small fuel assembly with electrical heater rods, INCONEL alloy 600 spacers, reference test, high temperature, 1987	Fuel heatup (temperatures) and damage, cladding oxidation, H_2 generation, CORA-2/high temperature
CORA-5	Small fuel assembly with electrical heater rods, Ag-In-Cd absorber, 1988	Fuel heatup (temperatures) and damage, cladding oxidation, H_2 generation, CORA-2/Ag-In-Cd absorber
CORA-7	Large (52 rods) fuel assembly with electrical heater rods; flow of steam and Ar through assembly, slow cooling, 1990	Fuel heatup (temperatures) and damage, cladding oxidation, H_2 generation, CORA-5/bundle size
CORA-9	Small fuel assembly with electrical heater rods, Ag-In-Cd absorber, 10-bar system pressure, 1989	Fuel heatup (temperatures) and damage, cladding oxidation, H_2 generation, CORA-5/system pressure

(Continued)

TABLE II (Continued)

Test/Accident	Description	Phenomena Tested
PWR		
CORA (Continued)		
CORA-10	Small fuel assembly with electrical heater rods, Ag-In-Cd absorber, low steam flow rate (2 g/s), 1992	Fuel heatup (temperatures) and damage, cladding oxidation, H_2 generation, CORA-5/steam flow rate (2 g/s versus standard of 12 g/s)
CORA-12	Small fuel assembly with electrical heater rods, Ag-In-Cd absorber, rapid quenching, 1988	Fuel heatup (temperatures) and damage, cladding oxidation, H_2 generation, CORA-5/quenching
CORA-13	Small electrically heated fuel assembly; flow of steam and Ar followed by rapid reflood (quenching) of hot assembly, 1990	Fuel heatup (temperatures) and damage, cladding oxidation, H_2 generation, quench behavior, OECD standard problem, CORA-12/quench at higher temperature
CORA-15	Small fuel assembly with electrical heater rods, Ag-In-Cd absorber, rods with high internal pressure, 1989	Fuel heatup (temperatures) and damage, cladding oxidation, H_2 generation, influence of clad ballooning and bursting
CORA-29	Small fuel assembly with electrical heater rods, Ag-In-Cd absorber, preoxidized cladding, 1991	Fuel heatup (temperatures) and damage, cladding oxidation, H_2 generation, CORA-5/preoxidation
CORA-30	Small fuel assembly with electrical heater rods, Ag-In-Cd absorber, slow heatup (0.2 K/s), 1991	Fuel heatup (temperatures) and damage, cladding oxidation, H_2 generation, CORA-5/heatup rate (0.2 K/s versus standard of 1 K/s)
PHEBUS		
B9+	Fuel assembly heatup and damage with steam flow followed by He to represent extreme steam starvation	Fuel heatup (temperatures), damage, and liquefaction, bundle collapse, eutectic behavior, cladding oxidation, H_2 generation
FPT-0	Fuel assembly heatup with steam flow	Fuel heatup (temperatures) and damage, cladding oxidation, H_2 generation
FPT-1	Integral severe fuel damage tests: fuel bundle, steam generator deposition, containment aerosol/chemistry	Fuel heatup (temperatures), damage, and liquefaction, bundle collapse, eutectic behavior, cladding oxidation, H_2 generation, fission product release, speciation and volatility, Ag aerosol transport and deposition, containment chemistry and deposition, and iodine partitioning
FPT-2	Integral severe fuel damage tests: fuel bundle, steam generator deposition, containment aerosol/chemistry—test includes steam-starved period	Fuel heatup (temperatures), damage, and liquefaction, bundle collapse, eutectic behavior, cladding oxidation, H_2 generation, fission product release, speciation and volatility, transport and deposition, containment chemistry and deposition, and iodine partitioning
FPT-3	Integral severe fuel damage tests: fuel bundle, steam generator deposition, containment aerosol/chemistry—test includes B_4C control rod	Fuel heatup (temperatures), damage, and liquefaction, bundle collapse, eutectic behavior, cladding oxidation, H_2 generation, fission product release, speciation and volatility, B_4C control rod oxidation transport and deposition, containment chemistry and deposition, and iodine partitioning

(Continued)

TABLE II (Continued)

Test/Accident	Description	Phenomena Tested
PWR		
PHEBUS (Continued)		
FPT-4	Melt progression in debris bed geometry with irradiated fuel	Late-phase melt progression and low-volatility fission product release
QUENCH		
QUENCH-01 through QUENCH-15	Small (20 to 30 rods) fuel assembly with electrical heater rods, Ag-In-Cd absorber (one test with B_4C control rod), one test with E110 cladding, two tests with advanced western cladding, remaining tests with Zircaloy-4 cladding, 1998–2009, Karlsruhe Institute für Technologie (KIT)	Fuel heatup (temperatures) and damage, cladding oxidation, H_2 generation, quenching
TMI-2 accident	Full-scale PWR accident	System pressure, RCS piping heatup and final state of reactor core; indirect measurement of H_2 production
BWR		
Annular Core Research Reactor Damage Fuel Tests		
DF-4	Small bundle test that included fuel, channel box, and stainless steel control blade with B_4C, 1986, SNL	Fuel heatup (temperatures), fuel damage, cladding oxidation, H_2 generation, B_4C-stainless steel eutectic interaction, fuel liquefaction, fuel rod collapse
CORA		
CORA-16	Small (18 rods) electrically heated fuel assembly, with channel walls and B_4C/stainless steel control blade; flow of steam and Ar, slow cooldown, 1988, KIT	Fuel heatup (temperatures), fuel damage, cladding oxidation, H_2 generation
CORA-17	Small electrically heated fuel assembly, with channel walls and B_4C/stainless steel control blade; flow of steam and Ar, followed by rapid reflood of hot assembly, 1989, KIT	Fuel heatup (temperatures), fuel damage, cladding oxidation, H_2 generation, CORA-16/quenching
CORA-18	Large (48 rods) electrically heated fuel assembly, with channel walls and B_4C/stainless steel control blade; flow of steam and Ar, slow cooldown, 1990, KIT	Fuel heatup (temperatures), fuel damage, cladding oxidation, H_2 generation, CORA-16/bundle size
CORA-28	Small electrically heated fuel assembly, with channel walls and B_4C/stainless steel control blade; flow of steam and Ar, slow cooldown, preoxidized cladding, 1992, KIT	Fuel heatup (temperatures), fuel damage, cladding oxidation, H_2 generation, CORA-16/preoxidized cladding
CORA-31	Small electrically heated fuel assembly, with channel walls and B_4C/stainless steel control blade; flow of steam and Ar, slow cooldown, slow initial heatup (~0.3 K/s), 1991, KIT	Fuel heatup (temperatures), fuel damage, cladding oxidation, H_2 generation, CORA-16/heatup rate (0.3 K/s versus 1 K/s)
CORA-33	Small electrically heated fuel assembly, with channel walls and B_4C/stainless steel control blade; dry core conditions, slow cooldown, 1992, KIT	Fuel heatup (temperatures), fuel damage, cladding oxidation, H_2 generation, CORA-31/steam-starved conditions

(Continued)

TABLE II (Continued)

Test/Accident	Description	Phenomena Tested
BWR		
Full-Length, High-Temperature		
FLHT-6	Heatup of full-length BWR fuel assembly; gradual boiloff of coolant; most severe of the FLHT tests, Pacific Northwest National Laboratory/National Research Universal (NRU) reactor	Boiloff rate, fuel heatup (temperatures) and damage, H_2 generation, noble gas release. NOTE: This test was never executed, assembly was fabricated and inserted in the NRU but was canceled by Canadian prime minister orders.
Ex-Reactor		
XR1-1 and XR1-2	Small fuel assembly, with channel walls and B_4C/stainless steel control blade, 1994, SNL	Full-scale section of a BWR core with all core plate region component structures (grids, tie plate, nose piece, fuel support piece, and core plate); response of lower core structures (~1 m) to prototypic relocating liquid materials from upper core
XR2-1	Large fuel assemblies (four represented with a total of 71 rods), with channel walls and B_4C/stainless steel control blade, 1996, SNL	Full-scale section of a BWR core with all core plate region component structures (grids, tie plate, nose piece, fuel support piece, and core plate); response of lower core structures (~1 m) to prototypic relocating liquid materials from upper core

*References 51 and 55 through 60.

product release under dry cavity conditions, as well as the effectiveness of coolant in terminating the MCCI by quenching the molten core material and rendering it permanently coolable. For the dry case, decay heat is continually dissipated by erosion of underlying concrete and can eventually lead to containment bypass by axial erosion through the extent of the concrete basemat. Conversely, for BWR containments, radial erosion can undermine essential support structures such as the reactor support pedestal. Aside from exacerbating fission product release, continued ablation can lead to containment pressurization by production of noncondensable gases arising from concrete decomposition. In addition, for scenarios in which the core debris contains unoxidized cladding and/or structural steel, generation of flammable gases (H_2 and CO) from the interaction of concrete decomposition gases (H_2O and CO_2) with metals present in the melt can also present a containment challenge. Cavity flooding offers the opportunity to quench the core debris and prevent basemat melt-through, greatly attenuate fission product release from core debris, and terminate containment pressurization by noncondensable gas production. If the core material that has relocated ex-vessel can be quenched and rendered permanently coolable by formation of sufficient porosity within the debris for water to ingress, then one significant aspect of the accident progression could be successfully halted. However, steam will continue to be generated as decay heat is removed from the debris. So, complete termination of the ex-vessel accident progression will inherently hinge upon maintaining adequate containment heat sink. Furthermore, the distribution of debris found within the TMI-2 RPV indicates that fuel is not always dispersed into the cavity at the same time during an accident. The quenching of relocated fuel released from a failed RPV does not preclude continued degradation and fission product release from fuel remaining in the core. These practical matters need to be factored into any evaluation of ex-vessel accident progression involving cavity flooding.

Based on the above-mentioned potential merits, ex-vessel corium coolability has been the focus of extensive research over the last 20 yr as a potential accident management strategy for current plants. In addition, outcomes from this research have impacted the accident management strategies for the Generation III+ LWR plant designs that are currently being deployed around the world. This section provides (a) a historical overview of corium coolability research, (b) a summary of the current status of research in this area, and (c) trends in SAM

TABLE III

Late-Phase Melt Behavior and RPV Failure Data

Test	Description	Phenomena Tested
RASPLAV (Refs. 62 and 63)		
AW-200-1 through AW-200-4	Prototypic material test with electrical heating to observe molten corium materials	Natural convection, stratification in molten pools
MASCA (Refs. 62 and 63)		
RCW-1 (RCW); MA-1 through MA-4 (RASPLAV-2)	Prototypic material test with electrical heating to observe stratification, natural convection, and fission product distribution in stratified corium materials	Natural convection, stratification, and fission product distribution in molten pools
FARO (Refs. 64, 65, and 66)		
L-5 to L-33	Prototypic materials relocating through water	Melt-water interactions, debris cooling, debris morphology, and debris-structure interactions
KROTOS (Refs. 67 through 70)		
K-21 to K-58	Prototypic materials poured into a water pool	Melt-water interactions, mixing and energetic vapor explosions
LHF/OLHF (Refs. 71 and 72)		
LHF-1 through LHF-6	One-fifth–scale test for predicting RPV failure with and without penetrations when subjected to well-defined electric heat load distributions	RPV and penetration failure
TMI-2 accident and postaccident examinations[5]	Full-scale PWR accident	Melt relocation, melt-water interactions, melt-structure interactions, RPV and penetration heatup

strategies that have evolved based on the findings from this work. Reviews of research in this area are primarily based on information in Refs. 43 and 73. Key data available for code assessment under dry cavity conditions are summarized in Table IV, while flooded cavity data are summarized in Table V.

Early pioneering studies[74,75] were conducted at Sandia National Laboratories (SNL) using steel melts to identify basic phenomenology associated with core-concrete interactions (CCIs). Subsequently, high-temperature sustained heating steel melt experiments were conducted under dry cavity conditions at SNL as part of the Sustained Urania Concrete (SURC) program to identify basic phenomenology associated with CCI. In particular, the SURC-3 and SURC-4 tests evaluated the effect of unoxidized cladding on the progression of CCI. These tests were followed by additional sustained heating experiments using metallic melts at Karlsruhe Institute of Technology (KIT) in the BETA and COMET test facilities in Germany. Recently, as part of the HECLA program, transient metal tests have been conducted at VTT in Finland that were focused on quantifying the ablation characteristics for hematite concrete, which is used as the sacrificial material in the reactor pit of the European Pressurized Reactor (EPR).

In terms of reactor material testing, a series of one-dimensional (1-D) experiments [Advanced Containment Experiment (ACE)/MCCI] addressing thermal-hydraulic behavior and fission product release was carried out at Argonne National Laboratory (ANL). In addition to these tests, several large-scale 1-D core melt tests (SURC) were

TABLE IV

Dry Cavity Melt-Concrete Interaction and Aerosol Generation Data

Program and Test(s)	Description	Phenomena Tested
SNL		
BURN-1 and large-scale transient tests	Early transient tests with molten stainless steel in concrete crucibles	Tests focused on identifying basic phenomenology associated with CCIs
ACE/MCCI		
L1-L2; L4-L6	Core oxide tests in 1-D cavities with direct electrical heating to simulate decay heat	Cavity erosion and fission product release of PWR and BWR melt compositions interacting with siliceous, LCS, serpentine, and limestone concretes
BETA		
V5.1 (ISP30)	Stainless steel tests in 2-D cavities with induction heating to simulate decay heat	Influence of Zircaloy cladding on cavity erosion behavior and aerosol release with siliceous concrete
COMET		
L2	Iron and Al_2O_3 in 2-D concrete cavities with induction heating to simulate decay heat	Cavity erosion and gas release for siliceous concrete
HECLA		
1-5	Transient stainless steel tests in 2-D cavities investigating initial transient cavity erosion phase	Cavity erosion for FeSi (hematite) concrete (used as sacrificial layer in the Olkiluoto 3 EPR reactor pit) as well as ordinary siliceous concrete
SURC		
QT-D, E; SURC-3, 3A, 4	Stainless steel tests in 1-D cavities with induction heating to simulate decay heat	Influence of Zircaloy cladding on cavity erosion behavior and aerosol release for LCS and siliceous concretes
1-2	Core oxide tests in 1-D cavities with induction heating of susceptor plates to simulate decay heat	Effect of Zircaloy cladding on cavity erosion and aerosol release from PWR melt composition interacting with LCS and basalt concretes
VULCANO		
VB-U1, U4-U7	Core oxide–stainless steel tests in 2-D cavities; induction heating to simulate decay heat	Cavity erosion for siliceous, LCS, and hematite concretes; focus on effect of stainless steel in corium

completed at SNL under both transient and sustained heating conditions. Two-dimensional (2-D) CCI experiments under dry cavity conditions have also been performed at the VULCANO test facility at Commissariat à l'énergie atomique et aux énergies alternatives (CEA) in France. Finally, a series of large-scale multidimensional CCI experiments was conducted as part of the internationally sponsored OECD/MCCI program at ANL that examined dry cavity erosion characteristics for several hours before the cavity was flooded.

These dry cavity results show that CCI during the early phase is influenced by the extent of unoxidized cladding that is initially present in the melt. However, the remaining cladding is rapidly oxidized within the

TABLE V

Flooded Cavity Melt-Concrete Interaction and Debris Coolability Data

Program and Test(s)	Description	Phenomena Tested
COMET		
L1, L3	Iron and Al_2O_3 in 2-D concrete cavities with induction heating to simulate decay heat	Cavity erosion and debris cooling rate for siliceous concrete
ECOKATS		
2	Large-scale transient spreading test with oxide simulant; flooded following spreading phase	Cavity erosion and debris cooling rate for siliceous concrete
COTELS		
B/C-2 to B/C-9	High power density core oxide tests in 2-D cavities with induction heating to simulate decay heat	Cavity erosion and the extent of debris quenching by the mechanisms of particle bed formation and water ingression into fragmented debris
MACE and OECD-MCCI		
MACE M0-M4; MCCI CCI 1-3 and SSWICS 1-7	Large scale, core oxide, prototypic power density tests in 1-D and 2-D cavities; direct electrical heating to simulate decay heat	Cavity erosion and debris cooling rate for LCS and siliceous concrete types; quantification of extent of cooling by melt eruption and water ingression mechanisms
SWISS		
1-2	Stainless steel tests in 1-D concrete cavities with induction heating to simulate decay heat	Cavity erosion, debris cooling rate, and aerosol scrubbing with melt interacting with LCS concrete
University of California, Santa Barbara (UCSB)		
15- to 120-cm test section spans	Glycerin–liquid N_2 tests with gas injection to simulate concrete decomposition gases	Debris cooling characteristics and morphology as a function of test section size
WETCOR		
1	Oxide simulant in 1-D concrete cavity with induction heating to simulate decay heat	Cavity erosion, debris cooling rate, and aerosol scrubbing with melt interacting with LCS concrete

first ~30 min of the interaction. During the long term, the nature of the CCI is found to be a strong function of concrete type. In particular, for siliceous concretes that release a low amount of water vapor and carbon dioxide gases upon decomposition, the radial/axial ablation is found to be strongly skewed radially. Conversely, for concretes that release a larger amount of gas upon decomposition, the radial/axial ablation rates are quite similar. Fission product release has also been investigated. For example, a range of parameters was addressed in one study[76] by a series of tests that used four types of concrete (siliceous, limestone/sand, serpentine, and limestone) and a range of metal oxidations for both BWR and PWR core debris. The released aerosols contained mainly constituents of the concrete. In the tests with metal and limestone/sand or siliceous concrete, silicon compounds comprised 50% or more of the aerosol mass. Releases of uranium and low-volatility fission product elements were small. Releases of tellurium and neutron absorber materials (silver, indium, and boron from boron carbide) were high. All these findings are consistent with predictions from the VANESA code.[77]

For wet cavity conditions, the research has focused on determining the effectiveness of water in terminating a CCI by flooding the interacting masses from above, thereby quenching the molten core debris and rendering it permanently coolable (Table V). As a part of this work, both simulant and reactor material experiments have been completed to provide a database to support model development and code validation activities. In particular, low-temperature simulant experiments were conducted at University of California Santa Barbara to identify the basic phenomenology associated with melt coolability, while high-temperature steel and oxide simulant experiments have been conducted at SNL as part of the SWISS and WETCOR programs to investigate coolability with concurrent concrete erosion. Large-scale steel and oxide simulant tests have also been conducted at KIT as part of the COMET and ECOKATS programs. In terms of reactor material testing, the COTELS, MACE, and OECD/MCCI programs have been completed to investigate the mechanisms of coolability under prototypic MCCI conditions. Depending upon melt composition and conditions, these various tests have revealed four mechanisms that can contribute to core debris quenching: (a) bulk cooling in which gas sparging is initially sufficient to preclude stable crust formation at the melt-water interface (and therefore, efficient heat transfer is achieved); (b) water ingression through fissures in the core material that augments what otherwise would be a conduction-limited cooling process; (c) melt (or volcanic) eruptions that lead to a highly porous overlying particle bed that is readily coolable; and (d) transient breach of crusts that form during the quench process, leading to water infiltration below the crust with a concurrent increase in the debris cooling rate.

Although the identified cooling mechanisms certainly increase the debris cooling rate, scaling effects in many of the tests have significantly influenced test outcomes, even at extremely large experiment scale at up to 2 tonnes of core melt mass. These occurrences have made it difficult to declare with certainty that a core melt can always be quenched under a wide range of conditions. On this basis, the research trend over the last several years has been to develop phenomenological models of the various cooling mechanisms observed in the tests in order to quantify the extent that these mechanisms can contribute to coolability. In terms of the water ingression cooling mechanism that is applicable to both in-vessel and ex-vessel conditions, fundamental modeling that considers the reactor material database has led to a correlation for the corium dryout heat flux.[78,79] The second major debris cooling mechanism that is applicable to ex-vessel conditions is melt eruptions. Motivated by eruptions observed in several reactor material tests in which up to 25% of the core debris was quenched and rendered coolable in the form of a porous particle bed,[73] several different modeling studies have been carried out at CEA, ANL, and the University of Wisconsin (Refs. 80 and 81, 82, and 83, respectively), in order to develop correlations for the melt entrainment coefficient that relate the melt ejection rate into overlying coolant to the melt gas sparging rate arising from concrete decomposition. The results of these modeling studies indicate that transformation into a quenched debris bed could be achieved for entrainment coefficients as low as 0.1% to 0.01% at atmospheric pressure.

These various phenomenological models are deployed in codes that are able to link the interrelated phenomenological effects, thereby allowing the results to be extrapolated to plant conditions. One such model (i.e., CORQUENCH; see Refs. 73 and 84) has been upgraded to include these findings, and the model was used to scope out an approximate debris coolability envelope for two concrete types. The results for limestone–common sand (LCS) concrete indicate that melt stabilization may be achievable in under 1 m of axial ablation as long as the cavity is flooded before the melt concrete content exceeds 15 wt% and the initial melt depth is $\leq$40 cm. Conversely, for siliceous concrete, stabilization may not be achieved in under 1 m of ablation unless the initial melt depth is fairly shallow (i.e., $\leq$20 cm) and the cavity is flooded before the melt concrete content exceeds 10 wt%. However, recent results from the OECD/MCCI program indicate that core melt over siliceous concrete can also be very coolable if the cavity is flooded before significant CCI commences. However, for preflooded cavity conditions it is important to consider the potential for coolant sweep-out due to steam countercurrent flow when high-temperature core melt relocates from the RPV into the cavity. Under these conditions, cavity geometry (and to a lesser extent, water inlet flow rate) will influence the rate at which coolant is able to reflood the debris.

These modeling studies have highlighted the need to implement ex-vessel debris cooling models into system-level codes such as MELCOR and MAAP in order to improve the fidelity of plant analyses for beyond-design-basis-accident sequences.

III.C. Summary

As discussed in this section, the development of integrated systems analysis tools containing models to simulate various severe accident phenomena is a long-term benefit from TMI-2 postaccident evaluations. Such tools are used for evaluating new plant designs, proposed accident management strategies, and proposed plant design changes. Many of the models developed within such modeling tools have been assessed against experimental test data or data obtained from the TMI-2 event and smaller-scale experiments. However, there clearly are gaps within the experimental database. As noted in Sec. IV, data from Units 1, 2, and 3 would not only reduce gaps in our knowledge about the events that occurred at Fukushima, but more importantly, the data offer an unprecedented opportunity to significantly reduce phenomenological uncertainties in severe accident progression.

IV. IMPORTANCE OF DATA FROM FUKUSHIMA EXAMINATIONS

Although the events at TMI-2 initially had many adverse effects on the U.S. nuclear industry, there clearly was a "silver lining." Once visual images confirmed that significant core damage had occurred, the industry and regulators made a concentrated effort to gain as much information as possible from the damaged plant. Ultimately, insights obtained from these efforts led to plant improvements that enhanced reactor safety, such as improved operator actions, improved accident response actions, improved control room design, and increased reliance on risk analysis.

Because of the potential benefits to reactor safety throughout the world, it is recommended that an international effort be formed that will develop a plan that identifies, to the extent possible, desired samples and information required from Units 1, 2, and 3 a priori. Rather than the "piecemeal" approach taken in the TMI-2 postaccident evaluation efforts, this integrated effort should develop a plan that would prioritize data needs and provide guidance related to the number, density (e.g., at every meter or every micrometer) and types of samples that should be extracted, and the types of analyses that should be completed. The feasibility of obtaining this information will need to be evaluated against practical considerations such as worker safety, equipment capabilities, and overall impact of cost on the decontamination and decommissioning effort. Countries participating in this effort would also help finance obtaining the data and completing associated analyses. It is recommended that this international effort be organized as soon as possible. To illustrate the types of information that may be of interest, we have presented our initial thoughts of the types of data that should be considered in this international effort.

Many aspects related to accident progression at Fukushima Daiichi Units 1, 2, and 3 are unknown (just as they were unknown after the accident at TMI-2). At this point, there are questions about the accuracy of data obtained from plant instrumentation during the accident, the effectiveness of accident mitigation strategies, the extent of core damage, the integrity of the RPV and containment, and the end state of the core materials. Clearly, data from examinations can address these questions, which is also of importance to the international community as it strives to reduce uncertainties in severe accident simulation codes.

As noted in Sec. III, available data for in-vessel and ex-vessel aspects of BWR accident progression are limited. Although there are some smaller-scale BWR fuel assembly fuel damage tests, there are no data for validating assumptions related to a full-core-melt accident, melt relocation, melt-debris interaction with the BWR core plate, and melt-debris interaction with the large volume of water and steel structures in the bottom head of a BWR or a skirt-supported BWR RPV failure. Furthermore, there are limited data from large-scale facilities for validating assumptions related to ex-vessel phenomena such as BWR containment liner failure. Although considerable experimental data have been obtained for predicting MCCI phenomena, issues remain related to their applicability in a full-scale PWR or BWR accident. Data obtained from Units 1, 2, and 3 offer the unique opportunity for resolving many modeling assumption validation issues or developing new models for phenomena not currently modeled in existing severe accident analysis tools such as the effect of salt on accident progression.[c]

Available information suggests that postaccident examinations could provide insights into the following in-vessel and RPV failure phenomena:

1. BWR fuel/clad and other core structures (channel walls and B_4C/stainless steel control blades) heatup and degradation
2. thermal loading and possible melting of core shroud and upper vessel internals
3. BWR melt relocation including the impact of melt-structure interactions, core plate holdup, and melt-water-structural interactions within the BWR bottom head
4. BWR lower head integrity, including possible penetration/weld damage and RPV failure
5. effect of structures in the cavity below the BWR lower head
6. impact of salt water addition (deposits on fuel and core structures, corrosion, fission product chemistry, etc.).

Similar to the manner in which the TMI-2 post-AEP unfolded, it is anticipated that additional phenomena will be identified as information is obtained from these damaged plants. For example, if the RPV(s) failed at Fukushima and core melt was discharged into the drywell(s), these reactors offer an unparalleled opportunity to gain insights into the following ex-vessel core melt progression and phenomenology:

1. Mark I containment failure
2. CCIs
3. core debris coolability.

The role of accident analyses, data from plant instrumentation, and operator notes and recollections throughout the postaccident evaluation activities should also be emphasized. As new insights are gained, it is important to compare plant analysis results that are based on available plant instrumentation (e.g., containment pressure,

[c]Although there are a limited number of U.S. plants that rely on saltwater as a backup for core cooling, many rely on freshwater, which also raises issues of corrosion and fission product chemistry.

RPV pressure, external vessel and piping temperatures, etc.), as well as information inferred from operator notes and recollections, and to update the analyses as needed. Obviously, if postaccident evaluations show that RPV failure occurred, plant analysis input should be examined and updated to reflect this observation.

Aside from the geometric details of the RPV, core, and containment and best estimates for coolant injection into the RPV and containment, information desired for postevent analyses includes

1. mass, geometry, and location of fuel, structures, and penetrations (both damaged and undamaged) within the RPV to better assess the extent of heatup and melting that occurred in each reactor
2. mass, composition, distribution, and morphology (e.g., particulate, previously molten cohesive mass with or without cracks, etc.), of relocated melt (including a depth profile of any relocated melt)
3. manner/location of core plate failure, melt interaction with the mass of RPV lower head structures
4. location and size of opening(s) in each RPV that led to any melt discharge (if any)
5. peak temperature of the melt pour stream (this admittedly is a difficult piece of information to discern, but nonetheless, it is important to estimate if possible to aid in spreading analyses) if the RPV has failed, the melt-debris interaction with the ex-vessel structures below the RPV
6. evidence of the presence/absence of water on the drywell floor at time of RPV failure (perhaps by evaluating the amount of degradation to the floor and the morphology of debris near the floor)
7. evidence that drywell head seals may have yielded during accident progression and allowed hydrogen to vent to the reactor building.

As noted in Sec. II, one of the principal safety questions evaluated for the Mark I containment after TMI-2 was the potential for the drywell steel liner to fail because of heating by corium that could spread from the pedestal region following failure of the RPV. Thus, the following information would be very helpful in terms of validating spreading models as well as MCCI ablation models:

1. mass, composition, morphology, and distribution within the drywell and annulus, which includes melt depth profile, particularly adjacent to the drywell shell if the melt spread that far
2. the location and size of any failure(s) in the drywell
3. ablation profile of the remaining concrete cavity.

If melt accumulations of more than a few centimeters deep existed within the drywell, then some degree of CCI could be expected. This information, coupled with the water injection flow rate data, would provide the opportunity to evaluate CCI models in relation to actual conditions that occurred at Fukushima.

In several of the above lists, the need for obtaining information about the morphology, depth, and composition of relocated core debris was identified. As outlined in Sec. III, prior research has provided evidence of two mechanisms that can augment ex-vessel coolability, namely, water ingression and melt eruptions. Thus, if a particle bed is discovered, then it would be beneficial to know the spatial distribution of the bed depth as well as particle size distributions as a function of the radial and axial locations within the bed. In addition, one would also like to know if the particles show evidence of "necking" or sintering. Other data that would be useful to glean include the overall mass of the particle bed, the characteristic composition of the bed that identifies core elemental constituents (U, Pu, Zr, Fe, B, Cr, and Ni), and other elements that would be introduced as a result of CCI (i.e., Si, Ca, and Mg). These data are useful in facilitating overall mass balances that can be used, e.g., to determine the mass of relocated core melt if the cavity ablation profile can be determined or, conversely, the amount of eroded concrete if the relocated melt mass can be determined but cavity erosion profile cannot.

If a cohesive layer of debris, or crust, with a thickness of $\sim$10 cm or more is found beneath the particle bed, then it is important to examine this cohesive layer for the following:

1. if the crust material contains a crack structure that would allow water to ingress and thereby augment coolability
2. the crust layer depth
3. the elemental composition within this crust layer.

Finally, after the core debris is recovered, it would be useful to know the cavity ablation profile, which is one of the computed results for CCI codes. This measurement would also provide the technical basis for assessing the fraction of the core decay heat that was dissipated through CCI, the balance of which would have been dissipated to the containment atmosphere during the accident.

As noted previously, the above items are provided as an example of data that could reduce uncertainties about the events at Fukushima and improve our general understanding of accident progression. Because of the potential benefits to reactor safety throughout the world, it is recommended that an international effort be formed as soon as possible to develop an integrated plan to identify and prioritize the types and density of data desired, the appropriate samples or examination locations for obtaining the desired data, and the appropriate evaluation techniques for evaluating such samples.

V. SUMMARY

The TMI-2 experience demonstrated that understanding the progression of the TMI-2 accident required plant instrumentation data, knowledge of operator actions taken during the event, analysis models, and postaccident inspections. Furthermore, TMI-2 postaccident examinations, in conjunction with data from smaller-scale experiments with well-defined conditions, significantly enhanced our understanding of severe accident phenomena.

Units 1, 2, and 3 offer a unique opportunity to gain similar understanding about BWR severe accident progression. To maximize the benefit from such an effort, we recommend that an international effort be organized as soon as possible to develop an integrated plan to identify and prioritize the types and density of data desired, the appropriate samples or examination locations for obtaining the desired data, and the appropriate evaluation techniques for evaluating such samples. Countries participating in this effort would also help finance obtaining the data and completing associated analyses.

ACKNOWLEDGMENTS

Idaho National Laboratory's work was supported by the DOE, Office of Nuclear Energy, under DOE-NE Idaho Operations Office contract DE-AC07-05ID14517, and ANL's work was supported by the DOE under contract DE-AC02-06CH11357. Oak Ridge National Laboratory is operated by UT-Battelle LLC under contract DE-AC05-00OR22725 with the DOE; SNL is a multiprogram laboratory operated by Sandia Corporation, Lockheed Martin Company, for the DOE National Nuclear Security Administration under contract DE-AC04-94AL85000.

REFERENCES

1. K. C. ROGERS, "Three Mile Island Reactor Pressure Vessel Investigations Project—Achievements and Significant Results," *Proc. Open Forum Sponsored by the OECD Nuclear Energy Agency and the U.S. Nuclear Regulatory Commission*, Boston, Massachusetts, October 20–22, 1993.

2. R. LONG, Testimony in "The American Experience: Meltdown at Three Mile Island," Public Broadcasting System Documentary (1999).

3. E. E. KINTNER, "After Three Mile Island Unit 2—A Decade of Change," *Nucl. Technol.*, **87**, 21 (1989).

4. W. PASEDAG, "DOE's TMI-2 Accident Evaluation Program," *Proc. Open Forum Sponsored by the OECD Nuclear Energy Agency and the U.S. Nuclear Regulatory Commission*, Boston, Massachusetts, October 20–22, 1993.

5. "Three Mile Island Reactor Pressure Vessel Investigation Project, Achievements and Significant Results," *Proc. Open Forum Sponsored by the OECD Nuclear Energy Agency and the U.S. Nuclear Regulatory Commission*, Boston, Massachusetts, October 20–22, 1993.

6. J. R. WOLF et al., "TMI-2 Vessel Investigation Project Integration Report," NUREG/CR-6197, U.S. Nuclear Regulatory Commission (1994).

7. J. S. WALKER, *Three Mile Island—A Nuclear Crisis in Historical Perspective*," University of California Press, Berkeley, California, and Los Angeles (2004).

8. J. HENDRIE, Testimony in "The American Experience: Meltdown at Three Mile Island," Public Broadcasting System Documentary (1999).

9. H. DENTON, Testimony in "The American Experience: Meltdown at Three Mile Island," Public Broadcasting System Documentary (1999).

10. P. HOFMANN et al., "Reactor Core Materials Interactions at Very High Temperatures," *Nucl. Technol.*, **87**, 146 (1989).

11. "Report of the Japanese Government to the IAEA Ministerial Conference on Nuclear Safety—The Accident at TEPCO's Fukushima Nuclear Power Stations," Government of Japan (June 2011).

12. "Additional Report of the Japanese Government to the IAEA—The Accident at TEPCO's Fukushima Nuclear Power Stations (Second Report)," Government of Japan (Sep. 2011).

13. D. N. CHIEN and D. J. HANSON, "Accident Management Information Needs for a BWR with a MARK I Containment," NUREG/CR-5702, U.S. Nuclear Regulatory Commission (1991).

14. "TEPCO Fukushima Update on March 29, 2012 [162]: 2nd Probing Inside the PCV of 1F-2," Tokyo Electric Power Company Web Site: http://www.tepco.co.jp/en/nu/fukushimanp/images/handouts_120326_07-e.pdf (current as of Mar. 29, 2012).

15. "Mid-and-Long-Term Roadmap Towards the Decommissioning of Fukushima Daiichi Nuclear Power Station Units 1–4," presented at Nuclear Emergency Response Headquarters, Government and TEPCO's Mid-to-Long Term Countermeasure Mtg., December 21, 2011; Tokyo Electric Power Company Web Site: http://www.tepco.co.jp/en/press/corpcom/release/betu11_e/images/111221e14.pdf (current as of Apr. 3, 2012).

16. R. E. HENRY, *TMI-2: An Event in Accident Management for Light-Water-Moderated Reactors*, American Nuclear Society, La Grange Park, Illinois (2011).

17. B. B. SCHNITZLER and J. B. BRIGGS, "TMI-2 Isotope Inventory Calculations," EGG-PBS-6798, EG&G Idaho, Inc., Idaho National Laboratory (1985).

18. D. W. GOLDEN et al., "Summary of the Three Mile Island Unit 2 Analysis Exercise," *Nucl. Technol.*, **87**, 326 (1989).

19. M. L. RUSSELL and R. K. McCARDELL, "Three Mile Island Unit 2 Core Geometry, *Nucl. Technol.*, **87**, 865 (1989).

20. R. RAINISCH, "Analysis of Gamma Scanning of In-Core Detector #18 (L-11) in Lower Reactor Vessel Head," TPO/TMI-175, GPU Nuclear Corporation (June 1985).

21. M. E. YANCEY, R. D. MEININGER, and L. A. HECKER, "TMI-2 In-Core Instrument Damage—An Update," GEND-INF-031, Vol. II, EG&G Idaho, Inc., Idaho National Laboratory (1984).

22. R. GOLD et al., "Solid State Track Recorder Neutron Dosimetry in the Three Mile Island Unit-2 Reactor Cavity," HEDL-7484, Westinghouse Hanford Company (1985).

23. V. R. FRICKE, "Core Debris Bed Probing," TPB 84-8, Rev. 1, GPU Nuclear Corporation (Feb. 1985).

24. E. L. TOLMAN et al., "TMI-2 Accident Scenario Update," EGG-TMI-7489, Idaho National Laboratory (1986).

25. J. M. BROUGHTON et al., "A Scenario of the Three Mile Island Unit 2 Accident," *Nucl. Technol.*, **87**, 34 (1989).

26. R. L. MOORE, D. W. GOLDEN, and E. L. TOLMAN, "Three Mile Island Unit 2 Degraded Core Heatup and Cooldown Analysis," *Nucl. Technol.*, **87**, 990 (1989).

27. D. J. N. TAYLOR, "TMI SPND Interpretation," *Proc. 1st Int. Information Mtg. TMI-2 Accident*, Germantown, Maryland, October 1985.

28. C. S. OLSEN, R. R. HOBBINS, and B. A. COOK, "Application of Severe Fuel Damage Experiments to Evaluating Three Mile Island Unit 2 Core Materials Behavior," *Nucl. Technol.*, **87**, 884 (1989).

29. A. D. KNIPE, S. A. PLOGER, and D. J. OSETEK, "PBF Severe Fuel Damage Scoping Test—Test Results Report," NUREG/CR-4683, U.S. Nuclear Regulatory Commission (1986).

30. J. P. ADAMS and R. P. SMITH, "TMI-2 Lower Plenum Video Data Summary," EGG-TMI-7429, Idaho National Laboratory (1987).

31. R. W. GARNER, D. E. OWEN, and M. R. MARTIN, "An Assessment of the TMI-2 Axial Power Shaping Rod Dynamic Test Results," GEND-INF-038, EG&G Idaho, Inc. (1983).

32. L. S. BELLER and H. L. BROWN, "Design and Operation of the Core Topography Data Acquisition System for TMI-2," GEND-INF-012, EG&G Idaho, Inc. (1984).

33. V. R. FRICKE, "Reactor Lower Head Video Inspection—Phase II," in "TMI-2 Technical Bulletin TB-86-3, Rev. 0," GPU Nuclear Corporation (Jan. 8, 1986).

34. A. M. RUBIN, "Overview and Organization of Three Mile Island Unit 2 Vessel Investigation Project," *Proc. Open Forum Sponsored by the OECD Nuclear Energy Agency and the U.S. Nuclear Regulatory Commission*, Boston, Massachusetts, October 20–22, 1993.

35. D. W. AKERS and B. K. SCHUETZ, "Physical and Radiochemical Examinations of Debris from the TMI-2 Lower Head," *Nucl. Safety*, **35**, *2*, 288 (1994).

36. N. COLE, T. FRIEDRICHS, and B. LIPFORD, "Specimens Removed from the Damaged TMI Reactor Vessel," *Proc. Open Forum Sponsored by the OECD Nuclear Energy Agency and the U.S. Nuclear Regulatory Commission*, Boston, Massachusetts, October 20–22, 1993.

37. D. R. DIERCKS and G. E. KORTH, "Results of Metallographic Examinations and Mechanical Tests of Pressure Vessel Samples from the TMI-2 Lower Head," *Nucl. Safety*, **35**, *2*, 301 (1994).

38. G. E. KORTH, "Peak Accident Temperatures of the TMI-2 Lower Pressure Vessel Head," *Proc. Open Forum Sponsored by the OECD Nuclear Energy Agency and the U.S. Nuclear Regulatory Commission*, Boston, Massachusetts, October 20–22, 1993.

39. D. R. DIERCKS and L. A. NEIMARK, "Mechanical Properties and Examination of Cracking in TMI-2 Pressure Vessel Lower Head Material," *Proc. Open Forum Sponsored by the OECD Nuclear Energy Agency and the U.S. Nuclear Regulatory Commission*, Boston, Massachusetts, October 20–22, 1993.

40. L. A. NEIMARK, "Insight into the TMI-2 Core Material Relocation Through Examination of Instrument Tube Nozzles," *Nucl. Safety*, **35**, *2*, 280 (1994).

41. E. L. TOLMAN, "TMI-2 Accident Evaluation Program," EGG-TMI-7048, Idaho National Laboratory (1986).

42. R. R. HOBBINS et al., "Review of Experimental Results on Light Water Reactor Core Melt Progression," *Nucl. Technol.*, **95**, 287 (1991).

43. B. R. SEHGAL, "Light Water Reactor (LWR) Safety," *Nucl. Eng. Technol.*, **38**, 697 (2006).

44. J. L. REMPE et al., "In-Vessel Retention of Molten Corium: Lessons Learned and Outstanding Issues," *Nucl. Technol.*, **161**, 210 (2008).

45. "MELCOR 1.8.5 User's Manual and MELCOR 1.8.5 Reference Manual," NUREG/CR-6119, Vols. 1, 2, and 3; Sandia National Laboratories: http://melcor.sandia.gov (current as of Apr. 2012).

46. "MAAP Modular Accident Analysis Program," Fauske and Associates; http://www.fauske.com/maap.html (current as of Apr. 2012).

47. Institute of Applied Energy, Ministry of Economy, Trade, and Industry (METI), IMPACT Project: http://www.iae.or.jp/e/group/safety_analysis.html (current as of Apr. 2012).

48. "ICARE/CATHARE: A Computer System Code for Analysis of Severe Accidents in LWRs," Commissariat à l'énergie atomique et aux énergies alternatives; http://wwwcathare.cea.fr/scripts/home/publigen/content/templates/show.asp?P=130&L=EN&SYNC=Y (current as of Apr. 2012).

49. "ATHLET-CD," Gesellschaft für Anlagen- und Reaktorsicherheit; http://www.grs.de/content/athlet-cd (current as of Apr. 2012).

50. M. S. VESHCHUNOV, A. E. KISELEV, and V. F. STRIZHOV, "Development of SVECHA Code for the Modelling of In-Vessel Phase of Severe Accident at Pressurized Water Reactors," *Izvestiya*, **2**, 6 (2004) (in Russian).

51. SCDAP/RELAP5-3D© CODE DEVELOPMENT TEAM, "SCDAP/RELAP5-3D© Code Manuals, Volumes 1–5," INEEL/EXT-02-00589, Rev. 2.2, Idaho National Laboratory (2003).

52. K. K. MURATA et al., "Code Manual for CONTAIN 2.0: A Computer Code for Nuclear Reactor Containment Analysis," NUREG/CR-6533, U.S. Nuclear Regulatory Commission (1997).

53. N. BIXLER, "Victoria 2.0: A Mechanistic Model for Radionuclide Behaviour in a Nuclear Reactor Coolant System Under Severe Accident Conditions," NUREG/CR-6131, U.S. Nuclear Regulatory Commission (1998).

54. J. KELLY et al., "Perspectives on Advanced Simulation for Nuclear Reactor Safety Applications," *Nucl. Sci. Eng.*, **168**, 128 (2011).

55. J. L. REMPE, "Test Data for US EPR Severe Accident Code Validation," INL/EXT-06-11326, Rev. 3, Idaho National Laboratory (May 2007).

56. P. HOFMANN et al., "Chemical-Physical Behavior of Light Water Reactor Core Components Tested Under Severe Reactor Accident Conditions in the CORA Facility," *Nucl. Technol.*, **118**, 200 (1997).

57. M. STEINBRUCK et al., "Synopsis and Outcome of the QUENCH Experimental Program," *Nucl. Eng. Des.*, **240**, 1714 (2010).

58. R. O. GAUNTT and L. L. HUMPHRIES, "Final Results of the XR2-1 BWR Metallic Melt Relocation Experiment," NUREG/CR-6527, U.S. Nuclear Regulatory Commission (1997).

59. R. D. GASSER, R. O. GAUNTT, and S. C. BOURCIER, "Late-Phase Melt Progression Experiment MP-1: Results and Analysis," NUREG/CR-5874, U.S. Nuclear Regulatory Commission (1996).

60. R. D. GASSER et al., "Late-Phase Melt Progression Experiment MP-2: Results and Analysis," NUREG/CR-6167, U.S. Nuclear Regulatory Commission (1996).

61. "Ability of Current Advanced Codes to Predict Core Degradation, Melt Progression, and Reflooding—Benchmark Exercise on an Alternative TMI-2 Accident Scenario," NEA/CSNI/R(2009) 3, Organisation for Economic Co-operation and Development/Nuclear Energy Agency/Committee on the Safety of Nuclear Installations (Aug. 2009).

62. "OECD MASCA Project: A Project to Investigate Chemical and Fission Product Effects on Thermal Loadings Imposed on the Reactor Vessel by a Convective Corium Pool During a Severe Accident," Russian Research Center Kurchatov Institute; Web Site: www.nsi.kiae.ru/Mbrief.htm (current as of Apr. 2012).

63. "CSNI/RASPLAV Seminar 2000, Summary and Conclusions," Munich, Germany, November 14–15, 2000, NEA/CSNI/R(2000)23, Organisation for Economic Co-operation and Development/Nuclear Energy Agency/Committee on the Safety of Nuclear Installations.

64. D. MAGALLON, I. HUHTINIEMI, and H. HOHMANN, "Lessons Learnt from FARO/TERMOS Corium Melt Quenching Experiments," *Nucl. Eng. Des.*, **189**, 223 (1999).

65. D. MAGALLON and I. HUHTINIEMI, "Corium Melt Quenching Tests at Low Pressure and Subcooled Water in FARO," *Nucl. Eng. Des.*," **204**, 369 (2001).

66. D. MAGALLON, "Characteristics of Corium Debris Bed Generated in Large-Scale Fuel-Coolant Interaction Experiments," *Nucl. Eng. Des.*, **236**, 1998 (2006).

67. H. HOHMANN et al., "FCI Experiments in the Aluminum Oxide/Water System," *Nucl. Eng. Des.*, **155**, 391 (1995).

68. I. HUHTINIEMI and D. MAGALLON, "Insight into Steam Explosions with Corium Melts in KROTOS," *Nucl. Eng. Des.*, **204**, 391 (2001).

69. I. HUHTINIEMI, D. MAGALLON, and H. HOHMANN, "Results of Recent KROTOS FCI Tests: Alumina Versus Corium Melts," *Nucl. Eng. Des.*, **189**, 379 (1999).

70. I. HUHTINIEMI, H. HOHMANN, and D. MAGALLON, "FCI Experiments in the Corium/Water System," *Nucl. Eng. Des.*, **177**, 339 (1997).

71. T. Y. CHU et al., "Lower Head Failure Experiments and Analyses," NUREG/CR-5582, U.S. Nuclear Regulatory Commission (1999).

72. L. L. HUMPHRIES et al., "OECD Lower Head Failure Project Final Report," OECD/NEA/CSNI/2, p. 27, Organisation for Economic Co-operation and Development/Nuclear Energy Agency/Committee on the Safety of Nuclear Installations (2002).

73. M. T. FARMER, D. J. KILSDONK, and R. W. AESCHLIMANN, "Corium Coolability Under Ex-Vessel Accident Conditions for LWRs," *Nucl. Eng. Technol.*, **41**, 575 (2009).

74. D. A. POWERS and F. E. ARELLANO, "Large-Scale, Transient Tests of the Interaction of Molten Steel with Concrete," NUREG/CR-2282, U.S. Nuclear Regulatory Commission (1982).

75. D. A. POWERS and F. E. ARELLANO, "Direct Observation of Melt Behavior During High Temperature Melt/Concrete Interactions," NUREG/CR-2283, U.S. Nuclear Regulatory Commission (1982).

76. J. K. FINK et al., "Aerosol and Melt Chemistry in the ACE Molten Core-Concrete Interaction Experiments," *High Temperature Mater. Sci.*, **33**, 51 (1995).

77. D. A. POWERS, J. E. BROCKMANN, and A. W. SHIVER, "VANESA: A Mechanistic Model of Radionuclide Release and Aerosol Generation During Core Debris Interactions with Concrete," NUREG/CR-4308, U.S. Nuclear Regulatory Commission (1986).

78. S. LOMPERSKI and M. T. FARMER, "Experimental Evaluation of the Water Ingression Mechanism for Corium Cooling," *Nucl. Eng. Des.*, **237**, 905 (2006).

79. S. LOMPERSKI, M. T. FARMER, and S. BASU, "Experimental Investigation of Corium Quenching at Elevated Pressure," *Nucl. Eng. Des.*, **236**, 2271 (2006).

80. J. M. BONNET and J. M. SEILER, "Coolability of Corium Spread onto Concrete Under Water, the PERCOLA Model," *Proc. 2nd CSNI Specialists' Mtg. Core Debris–Concrete Interactions*, Karlsruhe, Germany, April 1–3, 1992, Committee on the Safety of Nuclear Installations.

81. B. TOURNIAIRE and J. M. SEILER, "Modeling of Viscous and Inviscid Fluid Ejection Through Orifices by Sparging Gas," *Proc. 2004 Int. Congress Advances in Nuclear Power Plants (ICAPP '04)*, Pittsburgh, Pennsylvania, June 13–17, 2004, American Nuclear Society (2004).

82. M. T. FARMER, "Phenomenological Modeling of the Melt Eruption Cooling Mechanism During Molten Corium Concrete Interaction (MCCI)," *Proc. 2006 Int. Congress Advances in Nuclear Power Plants (ICAPP '06)*, Reno, Nevada, June 4–8, 2006, American Nuclear Society (2006).

83. K. R. ROBB and M. L. CORRADINI, "Melt Eruption Modeling for MCCI Simulations," *Proc. 14th Int. Topl. Mtg. Nuclear Reactor Thermal-Hydraulics (NURETH-14)*, Toronto, Canada, September 25–30, 2011.

84. K. R. ROBB and M. L. CORRADINI, "Ex-Vessel Corium Coolability Sensitivity Study with CORQUENCH Code," *Proc. 13th Int. Topl. Mtg. Nuclear Reactor Thermal-Hydraulics (NURETH-13)*, Kanazawa, Japan, September 27–October 2, 2009.